Efficiency of a regenerative direct-drive electromagnetic active suspension

Bart L.J. Gysen, Tom P.J. van der Sande, Johan J.H. Paulides and Elena A. Lomonova
Faculty of Electrical Engineering
Eindhoven University of Technology
Eindhoven, The Netherlands
Email: b.l.j.gysen@tue.nl

***Abstract*—The efficiency of a given direct-drive electromagnetic active suspension system for automotive applications is investigated. A McPherson suspension system is considered where the strut consists of a direct-drive brushless permanent magnet tubular actuator in parallel with a passive spring and damper. This suspension system has besides delivering active forces the possibility of regenerating power due to imposed movements. An LQR controller is developed for improvement of comfort and handling (dynamic tire load). Finally, the overall efficiency of the system is simulated for various road profiles.**

I. Introduction

The current and future trend in the automotive industry is towards commercializing hybrid and full electrical vehicles. One of the examples in this trend is the in-wheel motors which have a high performance, increased efficiency, innecessity of mechanical gears, flexibility and save space at the sprung mass for the placement of e.g. a battery pack [1]. Apart from all the improvements, this technology has a major drawback, it is shown that the comfort and stability drastically decreases due to the increase in unsprung to sprung mass ratio [2]. The in-wheel motors allow the degree of freedom to control traction and braking forces independently [3], however, improving comfort is extremely difficult. Therefore, an active suspension system will be necessary for successful implementation of these systems.

Electromagnetic active suspension systems are becoming increasingly attractive replacements for currently installed passive, semi-active and hydraulic active suspension systems due to the improvement in efficiency and decreasing costs. Research proved that the limited force density of an electromagnetic system compared to a hydraulic system can be overcome by proper choice of design, geometrical optimization and materials resulting in a relatively high force density of 663 kN/m^3, [4]. Even more, the ability of regeneration, allthough limited [5], and the innecessesity of continuous power compared to a hydraulic system make these systems more suitable due to the importance of reduced CO_2 emissions. Finally, these systems offer an increased bandwidth of about a factor 10 relative to hydraulics and pneumatics which drastically improves the performance with regard to comfort, stability and flexibility of full vehicle control.

This paper investigates the efficiency of a direct-drive electromagnetic active suspension system which consists of a coil spring in parallel with a brushless tubular permanent magnet actuator, [2], [4], [6], [7]. Due to its high force density, ideally zero attraction force, tubular structure, innecessity of mechanical gearbox, it is an excellent candidate for providing active forces within a very short response time. Furthermore, it can transfer linear motion directly into electrical energy, decreasing the overall power consumption. In Section II, the topology and specification of the electromagnetic suspension system are given. The criteria for comfort, tire load and suspension travel are defined and based upon the performance of the passive suspension system of the BMW 530i in Section III. Furthermore, an LQR controller is developed for these specifications. Section IV shows the simulation results for all the criteria which gives an overview of the overall power consumption and efficiency. Finally, conclusions are drawn in Section V.

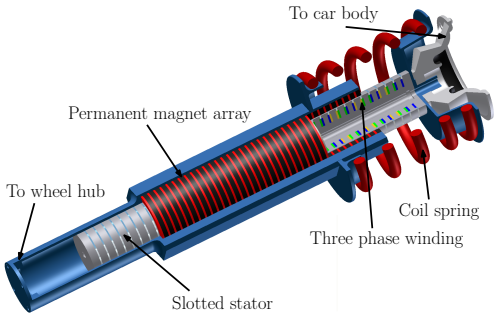

Fig. 1. Electromagnetic active suspension system.

II. Electromagnetic suspension system

The volumetric specifications are taken such that a retrofit on a BMW 530i is possible. The passive strut of the McPherson suspension will be replaced by the electromagnetic suspension system shown in Fig. 1. It consists of a passive coil spring for supporting the sprung mass and in parallel a direct-drive brushless tubular permanent actuator. Concerning safety, the suspension system should be able to provide damping when a power breakdown occurs, hence, a passive damper, d_p should be incorporated into the active suspension system. This can be obtained by means of an oil-filled damper in parallel, or electromagnetically by means of eddy currents.

978-1-4244-8218-4/10/$26.00 ©2010 IEEE

TABLE I
PARAMETERS OF THE TPMA

Parameter	Value	Description
R_{ph}	1.7 Ω	Phase resistance
L_{ph}	10 mH	Phase inductance
K_i	185 N/A	Motor constant upto $F_{act} = 1500$ N
K_e	123.3 Vs/m	EMF constant
F_{RMS}	1 kN	RMS force
F_{peak}	5 kN	Peak force
z_{max}	80 mm	Maximum rebound stroke
z_{min}	60 mm	Maximum bound stroke
τ_p	7.7 mm	Magnetic pole pitch

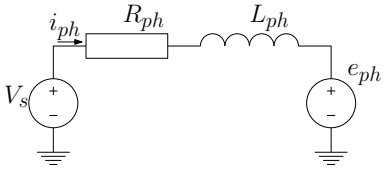

Fig. 2. Circuit diagram of one phase leg.

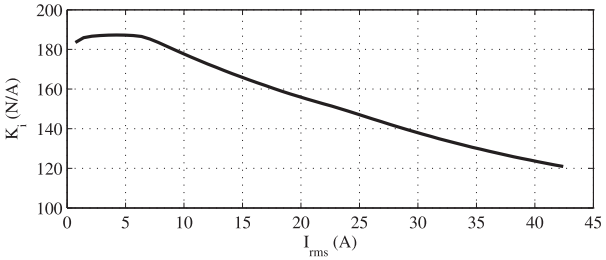

Fig. 3. Motor constant as function of the rms phase current.

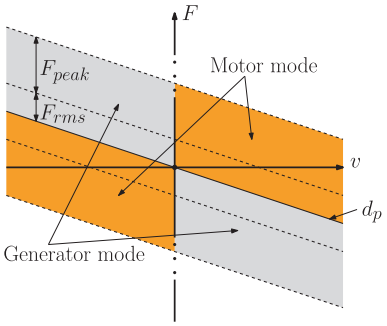

Fig. 4. Force velocity characteristic with various modes of operation.

The question is what the amount of passive damping should be in order to have an efficient system given certain specifications for comfort, tire load and suspension travel. In general, a lower passive damping will increase the ability of regenerating power since the actuator has to perform the 'damping' function, however, the safety decreases since less passive damping is present when a power breakdown occurs.

This suspension system is already optimized and designed in [4]. This resulted in the TPMA having the permanent magnets on the outer tube and a three phase slotted stator as the inner tube. The permanent magnet array is attached to the wheel hub via an aluminum housing. The slotted stator with a three phase winding topology is attached to the car body, hence, moving wires are avoided. The actuator is designed for minimal copper losses for a mean output force of 1 kN. The parameters of the final design are summarized in Table I.

The 12V battery of common passenger cars is not considered to be a limit since the development in the automotive industry is towards higher voltage levels, especially in hybrid and full electrical vehicles. The actuator will be driven by means of a PWM current controlled three phase amplifier with a DC bus voltage level of 340 V. Hence, with an EMF constant, K_e, of 123.3 Vs/m, the speed v can reach up to 2.75 m/s which is beyond the maximum speeds occurring in the suspension system, [2]. The amplifier has the possibility of providing a three phase current i_{ph} of 30 A rms and 60 A peak. The axial output force of the actuator will be modeled as $F_{act} = K_i\hat{i}$, where $\hat{i}$ is the amplitude of the three phase commutated current

$$i_a = \hat{i}\cos(\frac{\pi z}{\tau_p} + \phi), \quad (1)$$

$$i_b = \hat{i}\cos(\frac{\pi z}{\tau_p} + \frac{2\pi}{3} + \phi), \quad (2)$$

$$i_c = \hat{i}\cos(\frac{\pi z}{\tau_p} + \frac{4\pi}{3} + \phi), \quad (3)$$

with ϕ the commutation angle and τ_p the pole pitch of the quasi Halbach array. Up to the desired mean force of 1 kN, the value of K_i is around 185 N/A, however beyond 1500 N, saturation occurs and the value of K_i decays as observed in Fig. 3. Since the scope of the paper is on the average power levels, opposed to transient dynamics, an ideal amplifier is assumed with an ideal current control. One phase leg of the circuit diagram is shown in Fig. 2 and the associated equations for the copper losses, P_{cu}, mechanical power, P_{me} and supply power, P_s, are given by

$$P_{cu} = \frac{1}{t_e}\int_0^{t_e}\frac{3}{2}R_{ph}\hat{i}^2 dt, \quad (4)$$

$$P_{me} = \frac{1}{t_e}\int_0^{t_e}\frac{3}{2}K_e v dt, \quad (5)$$

$$P_s = \frac{1}{t_e}\int_0^{t_e}\frac{3}{2}V_s\hat{i} dt, \quad (6)$$

$$V_s = \hat{i}R_{ph} + L_{ph}\frac{\delta\hat{i}}{\delta t} + K_e v. \quad (7)$$

Inherently, the TPMA will have eddy current losses which will result in damping forces, however, these are not considered as 'losses' since they contribute to the value of the passive damping, d_p.

Since the suspension system can work in four quadrant operation, the passive damping d_p can be decreased (motor mode) as well as increased (generator mode), see Fig. 4.

The efficiency of an electromechanical servo system is generally defined as the ratio between the effective delivered mechanical power to the total input power. However, for an electromagnetic suspension system, working in four quadrant operation, the mechanical output power is not necessarily

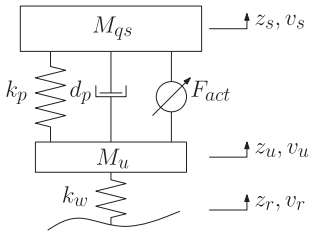

Fig. 5. Quarter car model.

TABLE II
PARAMETERS OF THE BMW 530I

Parameter	Value	Description
M_s	1500 kg	Sprung mass
M_u	45 kg	Unprung mass
k_p	30 N/mm	Coil spring stiffness
k_w	350 N/mm	Tire stiffness

'effective' or 'useful' output power. Different cases have to be considered:

- $P_{me} < 0$ and $P_s < 0$: The actuator works in generator mode and partially delivers power to the DC bus, hence the efficiency is defined as: $\eta = \dfrac{P_s}{P_{me}}$.
- $P_{me} > 0$ and $P_s > 0$: The actuator works in motor mode, the DC bus partially delivers power to the actuator, hence the efficiency is defined as: $\eta = -\dfrac{P_{me}}{P_s}$. The efficiency is defined negative since energy is delivered by the battery.
- $P_{me} < 0$ and $P_s > 0$: The actuator works in generator mode and the DC bus delivers power, this situation occurs when extreme damping is necessary. The regenerated power as well as the supply power are dissipated as copper losses, hence the efficiency is zero.
- $P_{me} > 0$ and $P_s < 0$: This situation never occurs.

III. MODELING AND CONTROL DESIGN

A quarter car model, shown in Fig. 5, is used to predict the actuator efficiency under the influence of road disturbances with the parameters given in Table II. For the control design, the motor constant is assumed to be fixed as indicated in Table I. The degrees of freedom are the vertical movement of the sprung (z_s) and unsprung mass (z_u). The road disturbance is typically modeled as a white noise disturbance with a first order filter [8]. The parameters of this filter depend on the road quality and vehicle speed. Fig. 6 shows the PSD of three typical road profiles together with the measurements for the smooth asphalt and rough pavement. The -2 slope can clearly be seen there. Typical road parameters are summarized in Table III.

The quarter car setup including road disturbances is generally modeled in state space as:

$$\dot{x} = Ax + Bu + Gw, \tag{8}$$

$$y = Cx + Du. \tag{9}$$

TABLE III
PARAMETERS OF THE ROAD PROFILES

Road type	a (rad/m)	σ_r (m)	v (m/s)
Smooth asphalt	0.05	0.4	30
Intermediate	0.2	0.5	20
Rough pavement	0.8	1.5	7.5

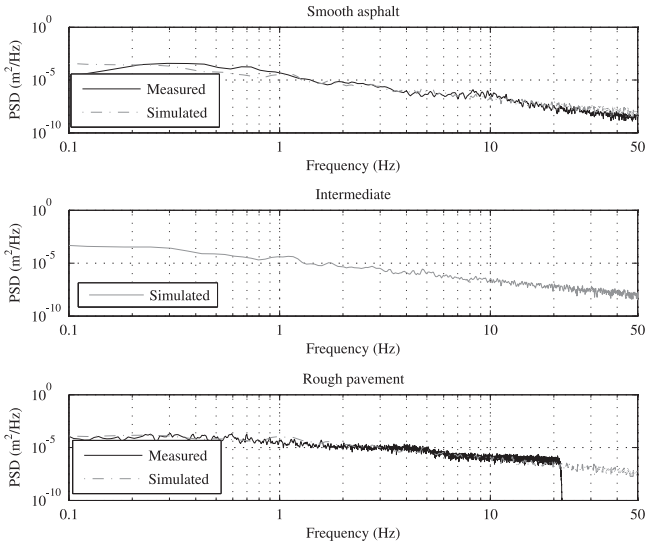

Fig. 6. PSD spectra of the simulated and measured road profiles.

With state vector

$$x = \begin{bmatrix} z_s & \dot{z}_s & z_u & \dot{z}_u & z_r \end{bmatrix}^T, \tag{10}$$

w is the white noise. Matrices A, B and G now become:

$$A = \begin{bmatrix} 0 & 1 & 0 & 0 & 0 \\ -\frac{k_s}{m_s} & -\frac{d_s}{m_s} & \frac{k_s}{m_s} & \frac{d_s}{m_s} & 0 \\ 0 & 0 & 0 & 1 & 0 \\ \frac{k_s}{m_u} & \frac{d_s}{m_u} & -\frac{k_s}{m_u} & -\frac{d_s}{m_u} & \frac{k_t}{m_u} \\ 0 & 0 & 0 & 0 & -av \end{bmatrix}, \tag{11}$$

$$B = \begin{bmatrix} 0 & \frac{1}{m_s} & 0 & -\frac{1}{m_s} & 0 \end{bmatrix}^T, \tag{12}$$

$$G = \begin{bmatrix} 0 & 0 & 0 & 0 & 1 \end{bmatrix}^T. \tag{13}$$

With matrices C and D the output variables are determined. Of interest here are the vehicle comfort and road holding with a constraint to suspension travel. This results in the following C and D matrices:

$$C = \begin{bmatrix} 0 & 0 & k_t & 0 & -k_t \\ -\frac{k_s}{m_s} & -\frac{d_s}{m_s} & \frac{k_s}{m_s} & \frac{d_s}{m_s} & 0 \\ 1 & 0 & -1 & 0 & 0 \end{bmatrix}, \tag{14}$$

$$D = \begin{bmatrix} 0 \\ \frac{1}{m_s} \\ 0 \end{bmatrix}. \tag{15}$$

Control of the active suspension is performed using an LQR controller, where it is assumed that the full state is measurable [9]. A quadratic weighting criterion is used such

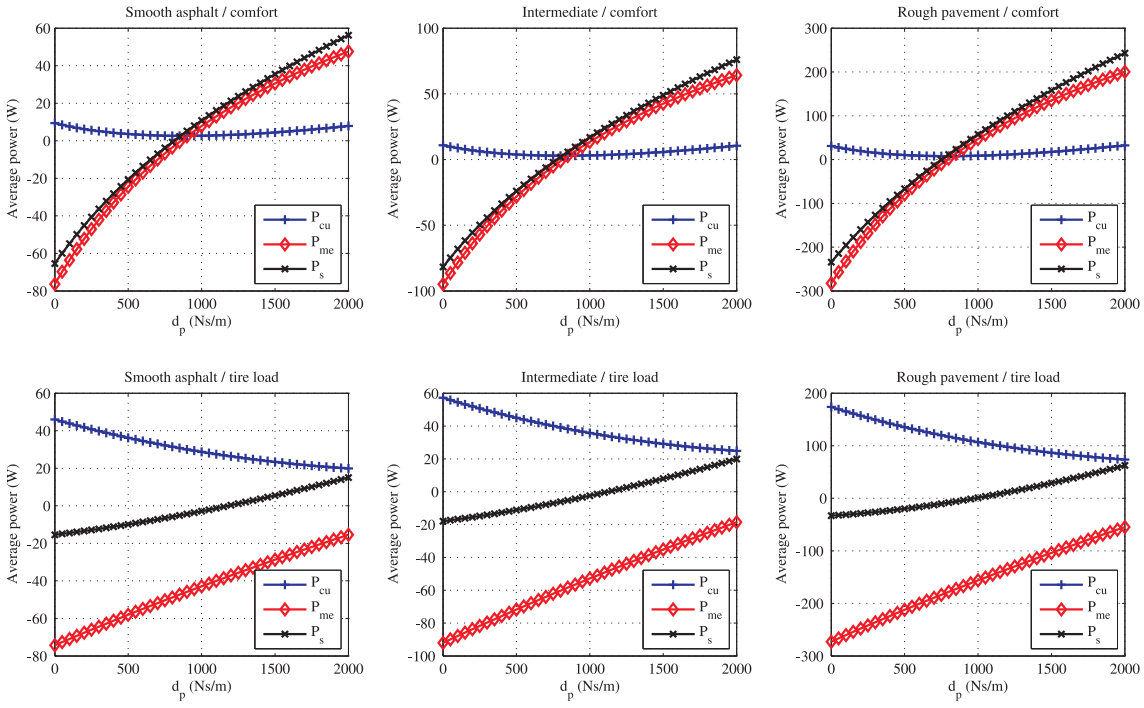

Fig. 7. Average power as a function of the passive damping for the various road / objective situations.

that, by choosing the weighting factors, one or two of the criteria can be emphasized. Furthermore, the actuator forces and speeds have to be within the specifications and the suspension travel is smaller or equal to the suspension travel of the passive strut for a fair comparison. The performance of the vehicle with passive suspension is summarized in Table IV. The criterion reads

$$J = \lim_{t_e \to \infty} \int_0^{t_e} (Cx + Du)^T Q (Cx + Du) \; dt = \int_0^{t_e} \begin{bmatrix} x^T & u^T \end{bmatrix} \begin{bmatrix} C^T Q C & C^T Q D \\ D^T Q C & D^T Q D \end{bmatrix} \begin{bmatrix} x \\ u \end{bmatrix} dt. \quad (16)$$

where Q is chosen to be a diagonal matrix containing the weighting factors. Variation calculus and differentiation leads to the state feedback [10]:

$$u(t) = -Kx, \quad (17)$$

with K

$$K = R^{-1} \left(N_c^T + B^T P \right). \quad (18)$$

and P the solution of the Riccati equation. The weighting factors contained in the matrix Q are summarized in Table V.

IV. Simulations

In total, six different situations are simulated and for every situation, the average mechanical power, supply power and copper losses are calculated depending on the chosen passive damping, d_p. The results are shown in Fig. 7 where it can be observed that concerning comfort, for increasing passive damping, the actuator works in generation mode when d_p is smaller than 800 Ns/m and in motor mode beyond. For the tire load objective, the actuator continuously works in generator mode, furthermore, the copper losses are significantly higher since greater actuator forces are necessary, see Fig. 10. The efficiency for the comfort and tire load objective is shown in Fig. 8 and Fig. 9, respectively. Since the damping power is linear dependent on the current whilst the copper losses are quadratically dependent on the current, there is an optimum for the generation mode for the comfort objective around $d_p = 250$ Ns/m with 86 %. The efficiency for the tire load objective are significantly lower due to the higher actuator forces. The improvement in comfort and dynamic tire load are shown in Table VI. In order to calculate the comfort, the sprung acceleration is weighted according to the ISO2631 criterion [11]. Since each controller in its turn focuses on either comfort or dynamic tire load, only an improvement on one of both criteria is expected. In general, the control design makes a trade-off between both criteria or apply adaptive control. Furthermore, the choice of d_p is close related to the fail-safe operation where a passive damping is necessary which will reduce the amount of regenerated power as can be observed in Fig. 7.

The optimal efficiency for the smooth road is chosen for

TABLE IV
Performance data of the passive BMW 530i suspension

Road	a_c (m/s^2)	z (mm)	F_t (N)
Smooth asphalt	1.099	6.719	852.5
Intermediate	1.191	7.277	959.1
Rough pavement	1.883	12.75	1737

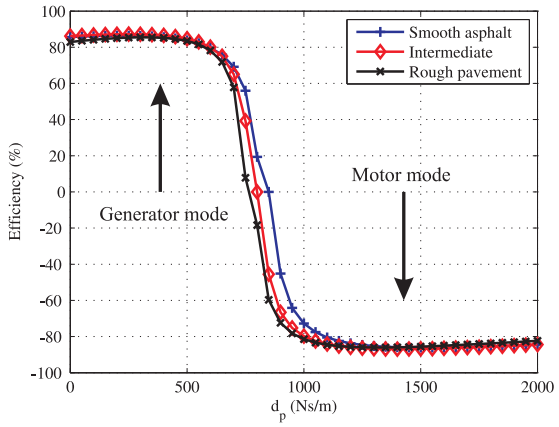

Fig. 8. Efficiency as a function of the passive damping for the comfort objective.

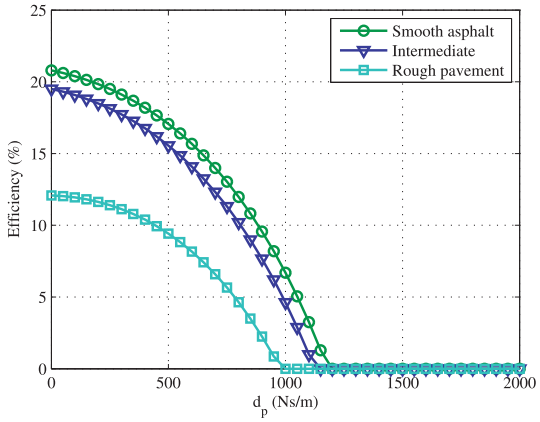

Fig. 9. Efficiency as a function of the passive damping for the tire load objective.

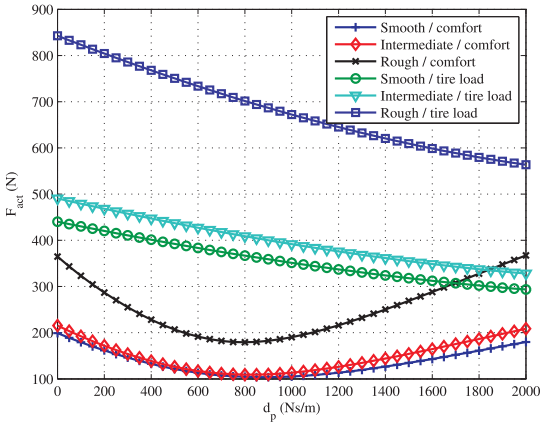

Fig. 10. Actuator force as a function of the passive damping for every situation.

both objectives, which is $d_p = 250$ Ns/m for comfort (Fig. 8) and $d_p = 0$ Ns/m for tire load reduction (Fig. 9). In Fig. 12 (a) the ISO weighted acceleration is shown for both objectives

TABLE V
WEIGHTING FACTORS

Situation	q_1	q_2	q_3
Comfort	5.85×10^{-7}	8.27×10^{4}	2.15×10^{9}
Tire load	5.85×10^{-5}	2.59	1.43×10^{5}

TABLE VI
IMPROVEMENT IN % FOR COMFORT AND DYNAMIC TIRE LOAD COMPARED TO THE PASSIVE SUSPENSION

Road / Obj.	max a_c	min a_c	max F_t	min F_t
Smooth / Comfort	43.958	27.416	-26.690	-77.344
Interm. / Comfort	45.492	27.614	-27.381	-78.901
Rough / Comfort	42.295	22.269	-22.485	-72.264
Smooth / Tire load	-11.991	-14.284	17.127	16.943
Interm. / Tire load	-14.759	-17.124	17.867	17.643
Rough / Tire load	-24.692	-27.656	21.716	21.268

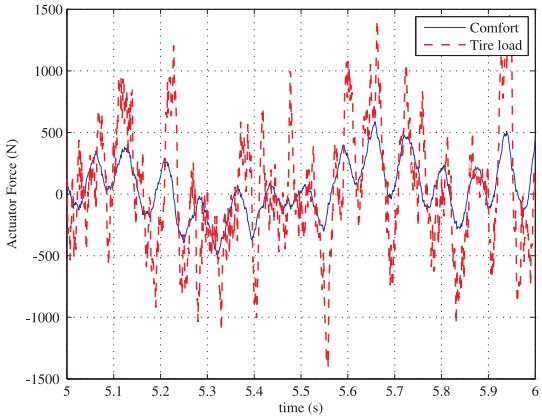

Fig. 11. Actuator force for $d_p = 250$ Ns/m emphasizing comfort and $d_p = 0$ Ns/m emphasizing dynamic tire load reduction.

together with the perfomance of the passive suspension system. Regarding the comfort objective, a reduction is obtained compared to the passive suspension performance. The dynamic tire load for both objectives is shown in Fig. 12 (b) together with the perfomance of the passive suspension system where an improvement is obtained when tire load reduction is emphasized.

Furthermore, a time plot of the required actuator forces is presented in Fig. 11 where it can be observed that the required performance of the actuator is higher for the tire load objective in terms of peak and rms force as well as bandwidth. Finally, the necessary supply power for both cases is shown in Fig. 13. More energy is obtained for the comfort objective, furthermore, the supply power for the tire load objective has much more high frequency content. This is explained by the fact that for the comfort objective the road input is filtered by the double mass-spring-damper system, whereas for reducing the tire load, the road vibrations act on the tire directly.

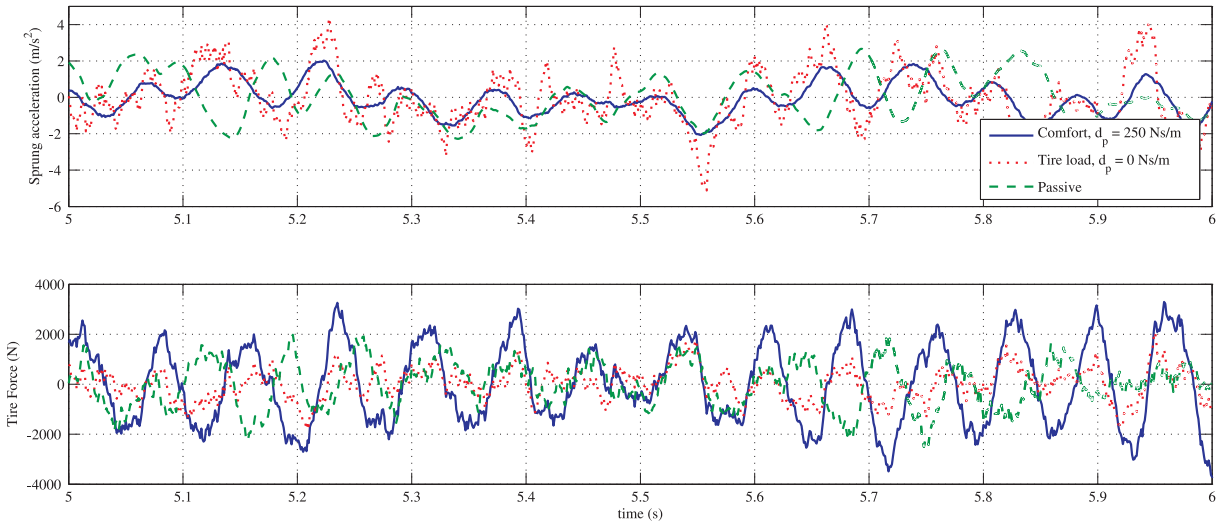

Fig. 12. (a) weighted body acceleration and (b) dynamic tire load of the active suspension system for $d_p = 250$ Ns/m emphasizing comfort and $d_p = 0$ Ns/m emphasizing dynamic tire load reduction together with the performance of the passive suspension system.

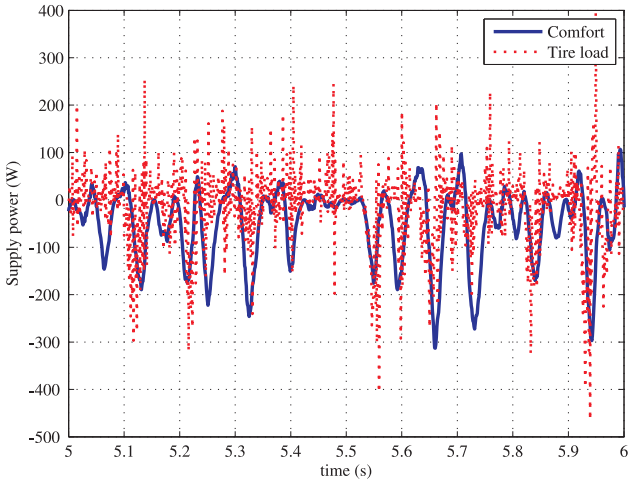

Fig. 13. Supply power for $d_p = 250$ Ns/m emphasizing comfort and $d_p = 0$ Ns/m emphasizing dynamic tire load reduction.

V. Conclusion

A direct-drive active suspension comprising a tubular PM actuator together with a coil spring is considered for the objectives of improvement of comfort or reduction of the dynamic tire load. The suspension system has the possibility of generating power as a result of the various road vibrations. Three different road profiles are defined based upon measurements and two LQR controllers are derived for both objectives. The efficiency for this electromechanical system is defined and simulated for the various situations. For safety reasons, a passive damping should be present, however this strongly influences the efficiency of the suspension system. For the comfort objective, power levels up to 235 W can be regenerated for a rough road and 65 W for a smooth road. Furthermore, higher power levels are obtained when emphasizing comfort.

Acknowledgment

The authors gratefully thank SKF for supporting this project.

References

[1] K. Cakir and A. Sabanovic, "In-wheel motor design for electric vehicles," *Advanced Motion Control, 2006. 9th IEEE International Workshop on*, pp. 613 –618, 2006.

[2] B. L. J. Gysen, J. J. H. Paulides, J. L. G. Janssen, and E. A. Lomonova, "Active electromagnetic suspension system for improved vehicle dynamics," *Vehicular Technology, IEEE Transactions on*, vol. 59, no. 3, pp. 1156 –1163, March 2010.

[3] B. Jacobsen, "Potential of electric wheel motors as new chassis actuators for vehicle manoeuvring," *Proceedings of the Institution of Mechanical Engineers, Part D: Journal of Automobile Engineering*, vol. 216, no. 8, pp. 631–640, March 2002.

[4] B. L. J. Gysen, J. J. H. Paulides, L. Encica, and E. A. Lomonova, "Slotted tubular permanent magnet actuator for active suspension systems," in *The 7th International Symposium on Linear Drives for Industry Applications, LDIA 2009*, Sept. 2009, pp. 292–295.

[5] P. Hsu, "Power recovery property of electrical active suspension systems," in *Energy Conversion Engineering Conference, 1996. IECEC 96. Proceedings of the 31st Intersociety*, vol. 3, 11-16 1996, pp. 1899 –1904 vol.3.

[6] B. L. J. Gysen, J. L. G. Janssen, J. J. H. Paulides, and E. A. Lomonova, "Design aspects of an active electromagnetic suspension system for automotive applications," *Industry Applications, IEEE Transactions on*, vol. 45, no. 5, pp. 1589–1597, Sept.-oct. 2009.

[7] J. Wang, W. Wang, K. Atallah, and D. Howe, "Comparative studies of linear permanent magnet motor topologies for active vehicle suspension," in *Vehicle Power and Propulsion Conference, 2008. VPPC '08. IEEE*, Sept. 2008, pp. 1–6.

[8] P. Michelberger, L. Palkovics, and J. Bokor, "Robust design of active suspension system," *Int. J. of Vehicle Design*, vol. 14, no. 2/3, pp. 145–165, 1993.

[9] M. M. Elmadany and Z. S. Abduljabbar, "Linear quadratic gaussian control of a quarter-car suspension," *Vehicle System Dynamics*, vol. 32, no. 6, pp. 479–497, 1999.

[10] H. Kwakernaak and R. Sivan, *Linear Optimal Control Systems*. United States of America: John Wiley and Sons Ltd, 1972.

[11] ISO, *ISO 2631-1:1997: Mechanical vibration and shock - Evaluation of human exposure to whole-body vibration*. Geneva - Switzerland: International Organization for Standardization, 1997.